PHYSICAL REVIEW C **82**, 051303(R) (2010)

Properties of triaxial, strongly deformed bands in ^{167}Ta and ^{167}Lu and the top-on-top model

Kazuko Sugawara-Tanabe[1,2,*] and Kosai Tanabe[1,3,†]
[1]*Theoretical Nuclear Physics Laboratory, RIKEN Nishina Center, Wako, Saitama 351-0198, Japan*
[2]*Otsuma Women's University, Tama, Tokyo 206-8540, Japan*
[3]*Department of Physics, Saitama University, Sakura-Ku, Saitama 338-8570, Japan*
(Received 30 August 2010; published 29 November 2010)

Based on the particle-rotor model with one particle coupled to a triaxially deformed rotor, the experimental excitation energy relative to a reference $E^* - aI(I+1)$ and the ratio between interband and intraband electromagnetic transitions are well reproduced for ^{167}Ta with $\gamma = 19^\circ$. The same parameter set for the angular-momentum-dependent rigid-body moments of inertia attains good agreement with experimental data for the positive-parity triaxial, strongly deformed (TSD) band levels in ^{167}Lu. An attempt is made to investigate the negative-parity TSD band in ^{167}Lu.

DOI: 10.1103/PhysRevC.82.051303 PACS number(s): 21.10.Re, 27.70.+q, 21.60.Ev, 23.20.−g

Starting from the particle-rotor model with one high-j nucleon coupled to a triaxially deformed core, we obtained an algebraic solution by introducing two kinds of bosons for the total angular momentum $\vec{I}$ and the single-particle angular momentum $\vec{j}$ in Ref. [1]. The core angular momentum $\vec{R} = \vec{I} - \vec{j}$ correlates with $\vec{j}$, and such an interplay between two tops with $\vec{R}$ and $\vec{j}$ is called the "top-on-top mechanism." In this model two kinds of quantum numbers describing precessions of $\vec{I}$ and $\vec{j}$, i.e., (n_α, n_β), classify the triaxial, strongly deformed (TSD) rotational bands. An important remark in Ref. [1] is that the next-to-leading order in the Holstein-Primakoff (HP) boson expansion is necessary for the restoration of the D_2 invariance [2], which reduces the number of independent bases necessary for the diagonalization to 1/4 of the full space. The formula for the $E2$ and $M1$ transition rates were also derived based on the top-on-top model in Ref. [1]. It has been demonstrated, in Refs. [1,3], that the hydrodynamical moments of inertia cannot explain the TSD bands even when the sign of the deformation parameter γ is changed. Furthermore, the detailed behavior of energy levels represented by the excitation energy relative to a reference, $E^* - aI(I+1)$ with $a = 0.0075$ MeV, is consistently reproduced by adoption of the angular-momentum dependence for the rigid-body moments of inertia, as well as the electromagnetic transition rates for TSD bands in odd-A Lu isotopes [4–8] with $\gamma = 17^\circ$. The angular-momentum dependence simulates the decrease of the pairing effect by a gradual increase of the core moments of inertia as a function of I.

The purpose of the present communication is to apply the angular-momentum dependence of moments of inertia to both isobars ^{167}Ta and ^{167}Lu with a common set of parameters to describe the energy levels and the ratios of $B(E2)_{\rm out}/B(E2)_{\rm in}$ observed by Hartley *et al.* [9]. The model Hamiltonian is given by

$$H = \sum_{k=x,y,z} A_k (I_k - j_k)^2 + \frac{V}{j(j+1)}\left[\cos\gamma\left(3j_z^2 - \vec{j}^2\right) - \sqrt{3}\sin\gamma\left(j_x^2 - j_y^2\right)\right], \tag{1}$$

where $A_k = 1/(2\mathcal{J}_k)$ $(k = 1, 2, 3$ or $x, y, z)$. We adopt the rigid-body moments of inertia,

$$\mathcal{J}_k = \frac{\mathcal{J}_0}{1 + \left(\frac{5}{16\pi}\right)^{1/2}\beta_2}\left[1 - \left(\frac{5}{4\pi}\right)^{1/2}\beta_2 \cos\left(\gamma + \frac{2}{3}\pi k\right)\right], \tag{2}$$

where β_2 and γ are the deformation parameters. The maximum moment of inertia is about the x axis, consistent with the largest oscillator strength in the x direction.

We choose the x axis as a quantization axis, and then a complete set of the D_2-invariant basis is given by

$$\left\{\sqrt{\frac{2I+1}{16\pi^2}}\left[\mathcal{D}^I_{MK}(\theta_i)\phi^j_\Omega + (-1)^{I-j}\mathcal{D}^I_{M-K}(\theta_i)\phi^j_{-\Omega}\right]; \quad K - \Omega = \text{even}, \quad \Omega > 0\right\}, \tag{3}$$

where K and Ω denote eigenvalues of I_x and j_x, respectively. The wave function ϕ^j_Ω stands for the spherical basis for the single-particle state, and $\mathcal{D}^I_{MK}(\theta_i)$ is the Wigner $\mathcal{D}$ function. The magnitude R of the rotor angular momentum $\vec{R} = \vec{I} + (-\vec{j})$ is restricted to $R = |I-j|, |I-j|+1, \ldots, I+j-1, I+j$, so that an integer n_β defined by $R = I - j + n_\beta$ ranges as

$$n_\beta = 0, 1, 2, \ldots, 2j-1, 2j. \tag{4}$$

Since R_x runs from R to $-R$, and $R_x = I_x - j_x = K - \Omega =$ even, an integer n_α defined by the relation $R_x = R - n_\alpha$ ranges as

$$\begin{aligned} n_\alpha &= 0, 2, 4, \ldots, 2R, \quad \text{for} \quad R = \text{even}, \\ n_\alpha &= 1, 3, 5, \ldots, 2R-1, \quad \text{for} \quad R = \text{odd}. \end{aligned} \tag{5}$$

Here we remark that the basis in Eq. (3) is the eigenstate of H for the case of $V = 0$ and $\gamma = \pi/3$ $(A_y = A_z)$, and the well-known eigenvalue of H for this case is given by

$$E_{\rm rot}(I, n_\alpha, n_\beta) = A_z R(R+1) - (A_z - A_x)(R - n_\alpha)^2. \tag{6}$$

Thus, a physical state is labeled by a set of non-negative integers (n_α, n_β).

*kazuko@kca.biglobe.ne.jp
†kosai@muj.biglobe.ne.jp

Keeping the same choice of quantization axis, we introduce the top-on-top model which takes into account the effect of Coriolis coupling in an algebraic way. Both angular momenta $\vec{I}$ and $\vec{j}$ are realized in terms of two kinds of HP boson operators $\hat{a}, \hat{a}^\dagger$ and $\hat{b}, \hat{b}^\dagger$ as follows:

$$\begin{aligned} I_+ &= I_-^\dagger = I_y + iI_z = -\hat{a}^\dagger\sqrt{2I - \hat{n}_a}, \\ I_x &= I - \hat{n}_a, \qquad \text{with} \quad \hat{n}_a = \hat{a}^\dagger\hat{a}; \end{aligned} \tag{7a}$$

$$\begin{aligned} j_+ &= j_-^\dagger = j_y + ij_z = \sqrt{2j - \hat{n}_b}\hat{b}, \\ j_x &= j - \hat{n}_b, \qquad \text{with} \quad \hat{n}_b = \hat{b}^\dagger\hat{b}. \end{aligned} \tag{7b}$$

Applying these HP representations to the Hamiltonian (1), we expand $\sqrt{2I - \hat{n}_a}$ and $\sqrt{2j - \hat{n}_b}$ into series in $\hat{n}_a/(2I)$ and $\hat{n}_b/(2j)$, and retain up to the next-to-leading order. The bosonized Hamiltonian obtained in such a way, H_B, restores the D_2 invariance as proved in Ref. [1]. Diagonalization of H_B is attained by the boson Bogoliubov transformation connecting HP boson operators $(\hat{a}, \hat{b}, \hat{a}^\dagger, \hat{b}^\dagger)$ to new boson operators $(\alpha, \beta, \alpha^\dagger, \beta^\dagger)$. Thus, an eigenvalue of H_B is expressed in terms of two kinds of quantum numbers, n_α and n_β. Here, n_α and n_β represent eigenvalues of $\hat{n}_\alpha = \alpha^\dagger\alpha$ and $\hat{n}_\beta = \beta^\dagger\beta$, respectively. Since the expression for the eigenvalue of H_B reduces to the one given by Eq. (6) in the limit of $V = 0$ and $\gamma = \pi/3$, eigenvalues of new boson operators coincide with integers n_α in Eq. (5) and n_β in Eq. (4). The physical contents of $\hat{n}_\alpha$ and $\hat{n}_\beta$ change, but they keep the same eigenvalues as in the symmetric limit whole through the adiabatic change of interaction parameter V and deformation parameters. Thus, the rotational bands can be classified in terms of a pair of quantum numbers (n_α, n_β) which is restricted by the D_2 invariance as in Eqs. (4) and (5).

Applying transformations in Eq. (7), we estimate the $E2$ and $M1$ transition rates approximately. We consider the overlap between the basis $|n_a n_b, Ij\rangle$ in the original HP boson picture and $|n_\alpha n_\beta, Ij\rangle$ in the new boson picture,

$$|n_\alpha n_\beta, Ij\rangle = \frac{1}{\sqrt{n_\alpha! n_\beta!}}(\alpha^\dagger)^{n_\alpha}(\beta^\dagger)^{n_\beta}|0\rangle_\alpha. \tag{8}$$

Then the overlap becomes

$$\begin{aligned} &G^{Ij}_{n_a,n_b;n_\alpha,n_\beta} \\ &\quad\equiv \frac{{}_a\langle 0|\hat{a}^{n_a}\hat{b}^{n_b}(\alpha^\dagger)^{n_\alpha}(\beta^\dagger)^{n_\beta}|0\rangle_\alpha}{(n_a! n_b! n_\alpha! n_\beta!)^{1/2}} \\ &\quad= \frac{{}_a\langle 0|0\rangle_\alpha}{(n_a! n_b! n_\alpha! n_\beta!)^{1/2}}\,{}_a\langle 0|\hat{a}^{n_a}\hat{b}^{n_b}(\hat{O})(\alpha^\dagger)^{n_\alpha}(\beta^\dagger)^{n_\beta}|0\rangle_\alpha, \end{aligned} \tag{9}$$

with $(\hat{O}) \equiv 1/{}_a\langle 0|0\rangle_\alpha$. In this expression, $n_a(= I - K)$ and $n_b(= j - \Omega)$ stand for the eigenvalues of $\hat{n}_a$ and $\hat{n}_b$, respectively. We notice that $G^{Ij}_{n_a,n_b;n_\alpha,n_\beta}$ is nonvanishing only when an integral value of $\Delta n \equiv n_a + n_b - n_\alpha - n_\beta$ is even. For simplicity, we employ an asymptotic estimation by assuming that I is large enough and the difference in the I dependence of $G^{Ij}_{n_a,n_b;n_\alpha,n_\beta}$ between initial and final states is negligible. We drop indices I and j from $G^{Ij}_{n_a,n_b;n_\alpha,n_\beta}$, and employ its abbreviation as $G_{n_a n_b n_\alpha n_\beta}$.

Here, we investigate the effect of Coriolis coupling on the $E2$ and $M1$ transition rates among TSD bands. We take the lowest-order contribution from the HP boson expansion for the case of $V = 0$. Then, the Bogoliubov transformation connecting HP boson operators $(\hat{a}, \hat{b}, \hat{a}^\dagger, \hat{b}^\dagger)$ to quasiboson operators $(\alpha, \beta, \alpha^\dagger, \beta^\dagger)$ is given by

$$\begin{pmatrix} \alpha \\ \beta \\ \alpha^\dagger \\ \beta^\dagger \end{pmatrix} = \begin{pmatrix} K & M \\ M & K \end{pmatrix} \begin{pmatrix} \hat{a} \\ \hat{b} \\ \hat{a}^\dagger \\ \hat{b}^\dagger \end{pmatrix}. \tag{10}$$

The submatrices are

$$K = \begin{pmatrix} \left(\frac{I}{I-j}\right)^{1/2}\eta_+ & -\left(\frac{j}{I-j}\right)^{1/2}\eta_- \\ 0 & \left(\frac{I}{I-j}\right)^{1/2} \end{pmatrix}, \tag{11a}$$

$$M = \begin{pmatrix} -\left(\frac{I}{I-j}\right)^{1/2}\eta_- & \left(\frac{j}{I-j}\right)^{1/2}\eta_+ \\ \left(\frac{j}{I-j}\right)^{1/2} & 0 \end{pmatrix}, \tag{11b}$$

with

$$\eta_\pm = \left\{ \begin{matrix} 1 \\ \mathrm{sign}(q-p) \end{matrix} \right\} \left[\frac{1}{2}\left(\frac{p+q}{2\sqrt{pq}} \pm 1\right)\right]^{1/2}, \tag{12}$$

where $p = A_y - A_x$ and $q = A_z - A_x$.[1] Thus, we obtain a few examples of $\Delta n = 0$ diagonal elements of G, which are referred to in the subsequent argument as

$$G_{0000} = \frac{1}{\sqrt{\det K}} = \left(\frac{I-j}{I}\right)^{1/2}\frac{1}{{\eta_+}^{1/2}}, \tag{13a}$$

$$G_{1010} = G_{0000}(K^{-1})_{11} = \frac{I-j}{I}\frac{1}{\eta_+^{3/2}}. \tag{13b}$$

In these expressions, the factor $\sqrt{(I-j)/I}$ arises from the effect of Coriolis coupling, which is not taken into account in Ref. [10]. We remark that only if we put $j = 0$, $G_{n_a n_b n_\alpha n_\beta}$ with the digits $n_b = n_\beta = 0$ reduces to $G_{n_a n_\alpha}$ [11–13], which is comparable with the case of "wobbling" in Ref. [10]. The approximate $B(E2)$ and $B(M1)$ values are summarized in tables and Figs. 1 and 2 in Ref. [3].

Diagonalization of H in Eq. (1) is carried out on the complete set of D_2-invariant bases with the same form as given by Eq. (3), but K and Ω denote the eigenvalues of I_z and j_z, respectively. The $E2$ and $M1$ transition operators are given by

$$\begin{aligned} \mathcal{M}(E2,\mu) &= \sqrt{\frac{5}{16\pi}}e\left[Q_0\mathcal{D}^2_{\mu 0} + Q_2\left(\mathcal{D}^2_{\mu 2} + \mathcal{D}^2_{\mu -2}\right)\right], \\ \mathcal{M}(M1,\mu) &= \sqrt{\frac{3}{4\pi}}\mu_N \sum_{\nu=0,\pm 1}\left[(g_\ell - g_R)j_\nu \right. \\ &\qquad \left. + (g_s - g_\ell)s_\nu + g_R I_\nu\right]\mathcal{D}^1_{\mu\nu}, \end{aligned} \tag{14}$$

[1] In Eq. (44c) in Ref. [1] and Eq. (22) in Ref. [3], $\mathrm{sgn}(p-q)$ should read $\mathrm{sgn}(q-p)$. These corrections do not affect any result in either paper. The formula in Eq. (12) holds through the range of $0 \leqslant \gamma \leqslant 2\pi/3$ for the case of rigid-body moments of inertia.

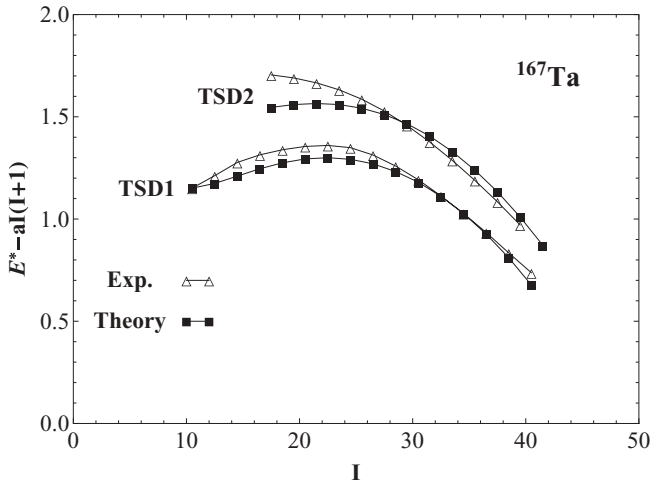

FIG. 1. Comparison between the experimental and the theoretical energy levels $E^* - aI(I+1)$ as functions of angular momentum I for ^{167}Ta. The vertical axis is in MeV. Theoretical values are shown as filled squares connected by solid lines, experimental values as open triangles connected by solid lines. The experimental data are from Ref. [9].

where $\mu_N = e\hbar/(2Mc)$, g_ℓ is the orbital g factor, g_s the spin g factor, and g_R the effective g factor for the rotational motion. The components of the intrinsic quadrupole moments, i.e., Q_0 and Q_2 are related with the deformation parameter γ through the relation

$$\frac{Q_2}{Q_0} = -\frac{\tan\gamma}{\sqrt{2}}, \tag{15}$$

which is consistent with the definition of H and $\mathcal{J}_k$ in Eqs. (1) and (2).

Generally, the experimental data for TSD bands [4–9] show some evolution with increasing I both in the excitation energy relative to a reference and the dynamical moment of inertia.

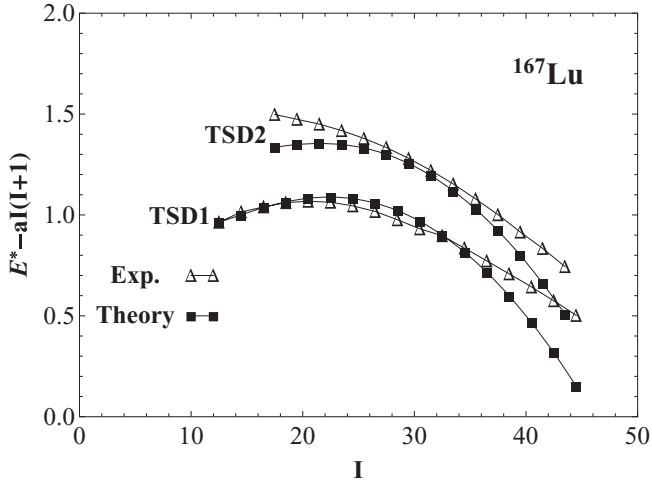

FIG. 2. Comparison between experimental and theoretical energy levels $E^* - aI(I+1)$ as functions of angular momentum I for ^{167}Lu. The vertical axis is in MeV. The meanings of the curves are as defined in Fig. 1. The experimental data are from Ref. [7].

These experimental results indicate there still remains the Coriolis antipairing (CAP) effect in the rotating core. As an attempt to reproduce the experimental energy levels, we simulate the effect of decreasing pairing on the moments of inertia in Eq. (2) simply by the replacement

$$\mathcal{J}_0 \to \mathcal{J}_0 \frac{I - c_1}{I + c_2}. \tag{16}$$

We call this formula by the angular-momentum dependence for the moments of inertia, and adopt $c_1 = 4.0$, $c_2 = 27.8$, and $\mathcal{J}_0 = 87.7$ MeV^{-1}. To reproduce not only energy levels but also $B(E2)_{\rm out}/B(E2)_{\rm in}$ for ^{167}Ta, we choose $\gamma = 19^\circ$ instead of 17°, and larger c_1 and c_2 values in comparison with the previous analysis in Ref. [3]. The other parameters are $V = 2.3$ MeV, $\beta_2 = 0.38$ in Eqs. (1) and (2), and $\pi i_{13/2}$ orbital is assumed for the positive-parity bands. Adopting these parameters, we carry out the exact diagonalization of the total Hamiltonian on the D_2-invariant basis to obtain the energy levels for each I. The precession quantum numbers can be assigned without ambiguity to the theoretical TSD bands, i.e., $(n_\alpha = 0, n_\beta = 0)$ for the TSD1 band and (1, 0) for the TSD2 band [1,3].

We compare theoretical energy levels of $E^* - aI(I+1)$ ($a = 0.0075$ MeV) with experimental ones for ^{167}Ta in Fig. 1, and for ^{167}Lu in Fig. 2. In these figures, theoretical values are shown as filled squares, experimental values as open triangles. Only the bandhead energy of (0,0) band is adjusted to the experimental bandhead energy of TSD1 in Figs. 1 and 2. Quite good fits to the experimental data are obtained over both nuclei. As for ^{167}Lu, the agreement with the experimental data becomes much better than in Fig. 7 in the previous paper [3], which adopts the same parameter set as ^{163}Lu at $\gamma = 17^\circ$.

We compare the theoretical ratio of $B(E2)_{\rm out}/B(E2)_{\rm in}$ with experimental data for ^{167}Ta [9] in Table I. In the third column, the theoretical prediction is given for the ratio of $B(M1)_{\rm out}/B(E2)_{\rm in}$. Quite good fit to the experimental values is obtained for $B(E2)_{\rm out}/B(E2)_{\rm in}$. As given by Eqs. (59a) and (59b) in Ref. [1], $B(E2)_{\rm out}/B(E2)_{\rm in}$ and $B(M1)_{\rm out}/B(E2)_{\rm in}$ for the transition from the TSD2 level become in the lowest-order approximation

$$\frac{B(E2)_{\rm out}}{B(E2)_{\rm in}} \equiv \frac{B(E2; I, 10 \to I-1, 00)}{B(E2; I, 10 \to I-2, 10)} \sim \frac{6}{I}\tan^2\left(\gamma + \frac{\pi}{6}\right)\left(\frac{G_{0000}}{G_{1010}}\right)^2, \tag{17}$$

TABLE I. Comparison of the theoretical ratio $B(E2)_{\rm out}/B(E2)_{\rm in}$ with the experimental [9] one for ^{167}Ta, and three different initial angular momenta I. The theoretical prediction of $B(M1)_{\rm out}/B(E2)_{\rm in}$ is also given.

I	$B(E2)_{\rm out}/B(E2)_{\rm in}$		$B(M1)_{\rm out}/B(E2)_{\rm in}$
	Expt.	Theory	Theory
39/2	0.37(4)	0.32	0.012
43/2	0.32(4)	0.29	0.011
47/2	0.36(4)	0.26	0.009

$$\frac{B(M1)_{\rm out}}{B(E2)_{\rm in}} \equiv \frac{B(M1; I, 10 \to I-1, 00)}{B(E2; I, 10 \to I-2, 10)} \sim \frac{16j^2}{5I}\left(\frac{\mu_N g_{\rm eff}}{eQ_0(\sqrt{3}-\tan\gamma)}\right)^2\left(\frac{G_{0000}}{G_{1010}}\right)^2, \quad (18)$$

where we put $g_{\rm eff} \equiv g_\ell - g_R + (g_s - g_\ell)/(2j) = 0.394$. As seen in Eq. (17), $B(E2)_{\rm out}/B(E2)_{\rm in}$ sensitively depends on γ through $\tan^2(\gamma + \pi/6)$, which makes us choose $\gamma = 19^\circ$ rather than 17°. The experimental data [9] also suggest $\gamma \sim 20^\circ$. As seen here in Table I and in Fig. 8 in Ref. [1], both theoretical ratios $B(E2)_{\rm out}/B(E2)_{\rm in}$ and $B(M1)_{\rm out}/B(E2)_{\rm in}$ decrease gradually with increasing I. Such a gradual decrease in both branching ratios are caused by a factor of $1/I$ in Eqs. (17) and (18). On the other hand, experimental data for both $B(E2)_{\rm out}/B(E2)_{\rm in}$ and $B(M1)_{\rm out}/B(E2)_{\rm in}$ show weak dependence on I. If γ increases very gradually with I, increase of the factors $\tan(\gamma + \pi/6)$ and $1/(\sqrt{3} - \tan\gamma)$ may compensate for the effect of $1/I$ in Eqs. (17) and (18).

For the negative-parity bands in ^{167}Lu, we test three cases of $j_{15/2}$, $h_{11/2}$, and $h_{9/2}$ orbitals for the valence proton. In reference to Eq. (5), the quantum number (0,0) is assigned to TSD3 for the cases of $j_{15/2}$ and $h_{11/2}$, while (1,0) for $h_{9/2}$. The set of parameters is the same as for the positive-parity bands both in ^{167}Ta and ^{167}Lu. Calculated level sequences for three cases are compared with the TSD3 levels in Fig. 3. Theoretical bandhead energies are shifted to the experimental one at $I = 25/2$. The spin dependence fits best to the experimental data for $j_{15/2}$, but it is unlikely from the viewpoint of relative single-particle energies between different orbitals, which are not taken into account in the model Hamiltonian of Eq. (1). In Fig. 3, we see that the spin dependence of the $h_{11/2}$ orbital becomes closer to the experimental curve at higher spin. In Ref. [3], we chose the $h_{11/2}$ orbital for the negative-parity band with different angular-momentum dependence of the core from the positive-parity band.

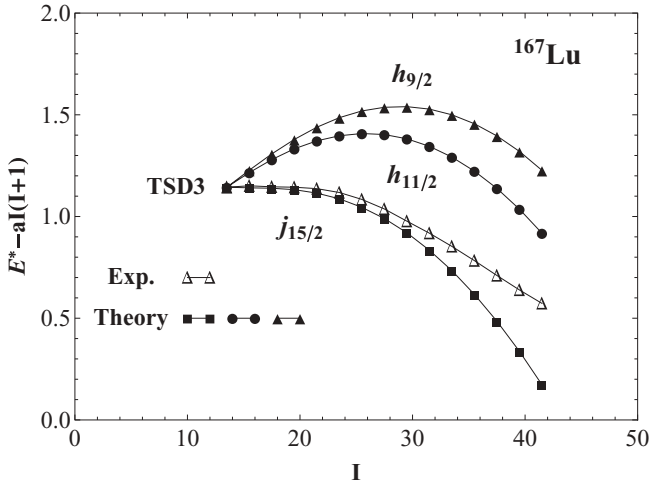

FIG. 3. Comparison of the theoretical energy levels $E^* - aI(I+1)$ for the negative-parity band assuming three cases of $j_{15/2}$, $h_{11/2}$, and $h_{9/2}$ as functions of angular momentum I with experimental energy levels in ^{167}Lu. The vertical axis is in MeV. The case with $j_{15/2}$ is shown by filled squares, $h_{11/2}$ by filled circles, and $h_{9/2}$ by filled triangles connected by solid lines. The experimental data [7] are open triangles connected by solid lines.

It is an interesting feature that all the positive- and negative-parity TSD band levels are basically well reproduced in terms of a common set of parameters in angular-momentum dependence for moments of inertia over the isobars with $A = 167$, i.e., ^{167}Ta and ^{167}Lu. This suggests that the CAP effect is caused by the $A = 166$ core taking part in the superfluidity.

As our simulation of experimental data is successful for odd-mass nuclei, it is quite natural to consider an extension of the same model and method to even-mass nuclei. Based on this model, we can give a possible answer to the question why TSD bands are not explicitly observed in even-even nuclei [14]. While several candidates of TSD bands with negative parity are observed in Hf isotopes, no interband transition between TSD1 and TSD2 is found. Let us imagine that two valence nucleons coupled to an even-mass TSD core occupy individual orbitals j_1 and j_2, respectively. If both angular momenta $\vec{j}_1$ and $\vec{j}_2$ are fully aligned to the rotational axis, and the sum $j = j_1 + j_2$ keeps constant over a relevant range of total angular momentum I, then the algebraic solution can be easily extended to an even-even nucleus with an alignment of integer j. In Eq. (3), ϕ^j_Ω is replaced by $\phi^{j_1}_{\Omega_1}\phi^{j_2}_{\Omega_2}$, and $K - \Omega$ by $K - \Omega_1 - \Omega_2$. Again the relevant space reduces to 1/4 of the full space because of D_2 invariance. For an integer j, $n_\beta = 0, 1, \ldots, 2j$ in Eq. (4), and there is no change in Eq. (5). Thus, even in even-A case, (0,0) is assigned to TSD1 and (1,0) to TSD2.

As seen from Tables II and IV in Ref. [3], we get for the $E2$ transition from TSD2 to TSD1,

$$B(E2; I, 10 \to I-1, 00) \sim \frac{3}{I}(Q_0' G_{0000} G_{1010})^2 \sim \frac{3}{I}(Q_0')^2\left(\frac{I-j}{I}\right)^3 \frac{1}{\eta_+^4}, \quad (19)$$

$$B(M1; I, 10 \to I-1, 00) \sim \frac{4j^2}{I}(G_{0000} G_{1010})^2 \sim \frac{4j^2}{I}\left(\frac{I-j}{I}\right)^3 \frac{1}{\eta_+^4}, \quad (20)$$

where $Q_0' = -\frac{1}{2}Q_0(1 + \sqrt{3}\tan\gamma)$. In deriving Eqs. (19) and (20), we used Eq. (13). The value of j is almost 14 due to the alignment of two particles in $i_{13/2}$ and $j_{15/2}$ orbitals for even-A nucleus, while the value of j in $i_{13/2}$ is 6.5 for odd-A nucleus. Then, $I - j$ is smaller for the even-A case than the odd-A case. For example, at $I = 18$ and $j = 14$, $[(I-j)/I]^3 \sim 0.011$ (even-A), while the ratio is 0.27 at $I = 37/2$ and $j = 6.5$ (odd-A), producing the ratio of B(even-A)/B(odd-A) ~0.04. In the ^{168}Hf case [15], the alignment seems to be much larger, like 23, resulting in a smaller value of $[(I-j)/I]^3$. This makes the observation of the other partner TSD band in the even-A nucleus more difficult. Further study about the even-A nucleus is in progress and will be published in a separate paper.

In conclusion, we have applied the particle-rotor model with the rigid-body moments of inertia assuming the angular-momentum dependence to the case of $A = 167$ isobars. The

angular-momentum dependence simulates the collapse of the pairing correlation in the rotating core. To explain both the energy level scheme and branching ratio observed in ^{167}Ta [9], we choose $\gamma = 19^\circ$ in accordance with experimental data. With the same set of parameters, we can explain positive-parity bands in ^{167}Lu. In both nuclei, an assumption that a valence proton occupies $i_{13/2}$ orbital is favorable for the positive-parity bands. Finally we make a conjecture as to why the interband transitions among TSD bands in the even-A nucleus are not yet identified. Under an assumption that the spin alignment of two single-particle levels is the sum of each j, and the sum keeps constant over some range of total angular momenta, the algebraic solution can be extended to an even-A nucleus. The rough estimate gives a factor of $[(I - j)/I]^3$ both in $B(E2)_{\rm out}$ and $B(M1)_{\rm out}$ values for the transition from (1,0) to (0,0). Comparing the case of $I = 18$ and $j = 14$ ($j_{15/2}$ and $i_{13/2}$) in even-A with the case of $I = 18.5$ and $j = 6.5$ ($i_{13/2}$) in odd-A, the ratio of B between even/odd reduces to 0.04. Such a reduction makes the observation of the transition between TSD1 and TSD2 bands in the even-A nucleus difficult.

We wish to acknowledge Professor Umesh Garg for his useful suggestions and encouragement throughout this work.

[1] K. Tanabe and K. Sugawara-Tanabe, Phys. Rev. C **73**, 034305 (2006); **75**, 059903(E) (2007).
[2] A. Bohr, Mat. Fys. Medd. K. Dan. Vidensk. Selsk. **26**, no. 14 (1952).
[3] K. Tanabe and K. Sugawara-Tanabe, Phys. Rev. C **77**, 064318 (2008).
[4] S. W. Ødegård *et al.*, Phys. Rev. Lett. **86**, 5866 (2001).
[5] D. R. Jensen *et al.*, Phys. Rev. Lett. **89**, 142503 (2002).
[6] G. Schönwaßer *et al.*, Phys. Lett. B **552**, 9 (2003).
[7] H. Amro *et al.*, Phys. Rev. C **71**, 011302 (2005).
[8] P. Bringel *et al.*, Phys. Rev. C **73**, 054314 (2006).
[9] D. J. Hartley *et al.*, Phys. Rev. C **80**, 041304(R) (2009).
[10] A. Bohr and B. R. Mottelson, *Nuclear Structure* (Benjamin, Reading, MA, 1975), Vol. II, Chap. 4.
[11] K. Tanabe and K. Sugawara-Tanabe, Phys. Lett. B **34**, 575 (1971).
[12] K. Tanabe, J. Math. Phys. **14**, 618 (1973).
[13] K. Sugawara-Tanabe and K. Tanabe, Nucl. Phys. A **208**, 317 (1973).
[14] G. B. Hagemann, Eur. Phys. J. A **20**, 183 (2004).
[15] R. B. Yadav *et al.*, Phys. Rev. C **78**, 044316 (2008).